

Fabrication of Organic Solar Cells from Surfactant-Free Aqueous Nanoparticle Dispersions

Karen Fischer, Florian Fichtelmann, Jan Bruder, Jonas Armleder, Holger Röhm, and Alexander Colsmann*

Light-harvesting layers in organic bulk-heterojunction solar cells are commonly fabricated from aromatic or even chlorinated solvents, which are often toxic or otherwise hazardous. In this work, nanoparticle dispersions of a blend of poly(3-hexylthiophene) and [6,6]-phenyl C₇₁-butric acid methyl ester (P3HT:PC₇₁BM) are synthesized in water, omitting any stabilizing surfactants which would remain in the layer and hamper the device performance. To overcome wetting issues and to master the deposition of thin films from aqueous dispersions, co-solvents are employed. The solar cells exhibit power conversion efficiencies of 2.7% and show excellent long-term stability, paving a promising way towards the all-eco-friendly production of organic solar cells in the future.

1. Introduction

The increasing appreciation of sustainability and legislation on the restriction of hazardous substances (RoHS) has fostered many innovations of eco-friendly production processes in industry. In particular, coating processes have undergone strong transformations from toxic and/or carcinogenic to less harmful media, examples of which include the development of water-based car finish or dispersant wall paints. Nowadays, the use of eco-friendly agents in coating processes is often industry standard, but of all things solar modules lag behind, although considered a sustainable technology in itself. Emerging photovoltaic technologies such as organic or perovskite solar cells are mostly deposited from solution, but the aromatic nature of the semiconductors commonly requires the use of aromatic or even chlorinated solvents which not only impose health risks during

industrial production on large scale but also entail solvent vapor capturing techniques that would drive up production costs.^[1]

If organic semiconductors are modified for solubility in water, which usually involves ionic functional side chains, their photovoltaic performance becomes insignificant. The literature also knows the alternative concept of water-based organic semiconductor dispersions which are very much in line with industrial requirements on coating processes, but the preeminent and unsolved problem is the so far non-negotiable use of surfactants to stabilize these aqueous dispersions.^[2,3] These sur-

factants attach to the surface of the organic (nano)particles with the polar end oriented toward the dispersant water, mimicking a surface charge and thus producing a repellent potential. Unfortunately, after thin-film deposition, the surfactants remain in the layer where they severely hamper the performance of solar cells.^[4]

More recently, surfactant-free organic nanoparticle dispersions of poly(3-hexylthiophene) (P3HT) were synthesized in ethanol. They were stabilized by the unique feature of P3HT to self-charge and thus to create an intrinsic electrostatic repellent potential.^[5]

In this work, we adopt the synthesis strategy of surfactant-free organic nanoparticle dispersions in ethanol and deploy the lessons learned to aqueous dispersions, moving further toward an all-eco-friendly solar cell production. We use the aqueous dispersions to fabricate organic solar cells and investigate their device stability.


2. Results and Discussion

2.1. Synthesis of Aqueous Nanoparticle Dispersions

For our study on the synthesis of surfactant-free aqueous nanoparticle dispersions, we have deliberately chosen bulk-heterojunctions comprising P3HT and either of the fullerenes indene-C₆₀ bisadduct (IC₆₀BA) or [6,6]-phenyl C₇₁-butric acid methyl ester (PC₇₁BM) at a polymer:fullerene ratio of 1:1 (w/w). While we appreciate recent more advanced co-polymer developments in the field of organic solar cells, P3HT distinguishes itself from all other polymers by being one of the very few polymers that form stable nanoparticle dispersions in alcohols through self-charging in the absence of any stabilization agents.^[5,6] Since in previous studies, the stabilization of the dispersion occurred

K. Fischer, F. Fichtelmann, J. Bruder, J. Armleder, H. Röhm, A. Colsmann
Material Research Center for Energy Systems
Karlsruhe Institute of Technology (KIT)
Strasse am Forum 7, 76131 Karlsruhe, Germany
E-mail: alexander.colsmann@kit.edu

K. Fischer, F. Fichtelmann, J. Bruder, J. Armleder, H. Röhm, A. Colsmann
Light Technology Institute
Karlsruhe Institute of Technology (KIT)
Engesserstrasse 13, 76131 Karlsruhe, Germany

 The ORCID identification number(s) for the author(s) of this article can be found under <https://doi.org/10.1002/ente.202500074>.

© 2025 The Author(s). Energy Technology published by Wiley-VCH GmbH. This is an open access article under the terms of the Creative Commons Attribution License, which permits use, distribution and reproduction in any medium, provided the original work is properly cited.

DOI: 10.1002/ente.202500074

only via the polymer, and therefore, the fullerene must be firmly embedded inside the polymer matrix, for our study, we chose the fullerenes IC₆₀BA and PC₇₁BM that are well miscible with the P3HT.^[7]

For the synthesis of the aqueous P3HT:fullerene dispersions, we used nanoprecipitation. For this purpose, we dissolved the P3HT:fullerene mixture in tetrahydrofuran (THF) at a concentration $c = 2 \text{ g L}^{-1}$ and then injected the solution into water. Since THF and water are miscible and P3HT is insoluble in water, the solubility of the organic semiconductors in the THF:water mixture is immediately reduced and nanoparticles are formed. Yet, we found that the particles synthesized along this route exhibited an average hydrodynamic diameter $d = 330 \pm 60 \text{ nm}$. These microparticles formed in water were much larger than their counterparts that were previously reported after nanoprecipitation from chloroform solution into ethanol ($d < 70 \text{ nm}$).^[8] We attribute this difference in size to the fact that THF and water mix much more slowly than chloroform and ethanol.^[9] Presumably, the slower mixing results in the formation of fewer polymer nuclei, which leads to fewer but larger nanoparticles.^[10] While aqueous P3HT:fullerene dispersions with larger particles were good to be used for catalytic hydrogen generation, the deposition of light-harvesting layers for solar cells with a projected thickness of 100 nm call for smaller nanoparticles.^[10]

To achieve sufficiently small nanoparticles in water, we revised the synthesis for nanoprecipitation in ethanol followed by re-dispersion in water as illustrated in **Figure 1**. Throughout this synthesis, we monitored the nanoparticle sizes, which are summarized in **Table 1**. First, we nanoprecipitated the P3HT:fullerene mixture from chloroform into ethanol, yielding nanoparticles with diameters of $d = 60 \pm 1 \text{ nm}$. After evaporation of the chloroform, we reduced the ethanol volume to recover the initial semiconductor concentration of $c = 2 \text{ g L}^{-1}$ without coagulation of the dispersions or other notable effects on the nanoparticle sizes. An aliquot of these dispersions in ethanol, which we set aside for reference, remained stable for more than 7 days. We note that the use of chloroform here does not conflict with the claim of eco-friendly processing, as the chloroform can be captured in a closed cycle in a chemistry environment during synthesis, which is all-different from chloroform evaporating during solar cell fabrication on large scale. Then we exchanged

the dispersant for water by re-dispersion of the nanoparticles, i.e., injection of the ethanol dispersion into water, evaporation of the ethanol and again recovery of the concentration of $c = 2 \text{ g L}^{-1}$ by evaporation of excess water (**Figure 1c and 1d**), without affecting the size of the nanoparticles. The contact angle of this dispersion on glass was identical to the contact angle of neat water and the absorbance of the dispersion in the infrared resembled the absorbance of pure water (**Figure S1, Supporting Information**) which is why we conclude that all ethanol was removed from the dispersion. The aqueous dispersions were stable for at least one day. After one week on the shelf, the aqueous P3HT:PC₇₁BM dispersion still maintained its stability whereas the P3HT:IC₆₀BA dispersion showed strong coagulation as reflected in the significantly larger nanoparticle sizes of 180 nm. Thus, when used immediately after synthesis, both dispersions are well suited for solar cell fabrication. However, if storage of the aqueous dispersion is required, P3HT:PC₇₁BM is the mixture of choice. We note that re-dispersion of the nanoparticles by drying and subsequent immersion in water, which is a common approach for inorganic nanoparticles, does not work with soft and “sticky” organic nanoparticles.

The question arose as to whether the synthesis including nanoprecipitation and subsequent re-dispersion could be simplified and combined into a single process. We tested this hypothesis by injecting chloroform solutions of the semiconductors into mixtures of ethanol and water at different concentrations, followed by evaporation of the chloroform and ethanol. However, this resulted in immediate phase separation of the solvent compounds and eventual coagulation of the dispersion, so we did not pursue this route any further.

2.2. Layer Formation and Wetting

The deposition of organic thin-films from aqueous dispersions is challenging in many ways: i) low semiconductor concentrations in dispersions require sequential multilayer deposition steps in order to obtain a sufficient layer thickness; ii) water is notorious for poor wetting of surfaces, in particular nonpolar surfaces, and the sequential multilayer deposition enhances this challenge; iii) after each deposition step, the layer must be dried in order to avoid uneven layer formation (e.g., by coffee ring effects).

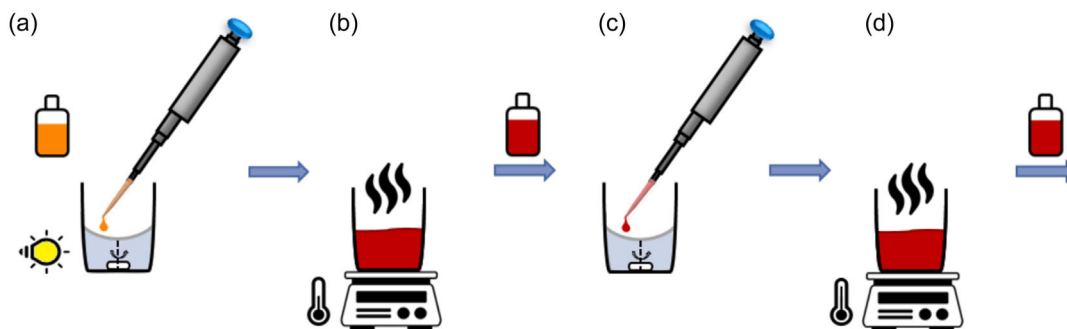


Figure 1. Synthesis of surfactant-free aqueous nanoparticle dispersions by nanoprecipitation. a) First, the organic semiconductors are dissolved in chloroform and then injected into ethanol under illumination. b) The chloroform is removed in a hot water bath and the initial semiconductor concentration of the solution recovered by evaporation of excess ethanol. c) Then the nanoparticle dispersion in ethanol is re-dispersed in water by injection into water. d) Finally, ethanol is thermally removed, again followed by the subsequent recovery of the initial semiconductor concentration by evaporation of excess water.

Table 1. Average nanoparticle (NP) sizes of P3HT:IC₆₀BA and P3HT:PC₇₁BM dispersions, monitored throughout their synthesis. An initial semiconductor concentration of $c = 2 \text{ g L}^{-1}$ in solution was chosen, with a P3HT:fullerene ratio of 1:1 (w/w). This semiconductor concentration was recovered in dispersion by volume reduction in ethanol and, later, in water.

Semi-conductors	NP size after nanoprecipitation, in ethanol [nm]	NP size after volume reduction, in ethanol [nm]	NP size after 7 days, in ethanol [nm]	NP size after volume reduction, in water [nm]	NP size after 1 day, in water [nm]	NP size after 7 days, in water [nm]
P3HT:IC ₆₀ BA (2 g L^{-1})	60 ± 1	63 ± 1	63 ± 1	60 ± 1	63 ± 1	180 ± 25
P3HT:PC ₇₁ BM (2 g L^{-1})	61 ± 1	64 ± 2	63 ± 1	67 ± 1	62 ± 1	67 ± 3

The comparably low semiconductor concentrations in surfactant-free dispersions in the g L^{-1} regime are a known issue from previous investigations of alcohol-based dispersions. In order to reduce the number of coating steps, we tested for higher concentrations of P3HT:PC₇₁BM than those used in Section 2.1. **Table 2** summarizes the long-term stability of aqueous P3HT:PC₇₁BM dispersions with concentrations of $c = 5\text{--}10 \text{ g L}^{-1}$ by monitoring the nanoparticle size over time in comparison to dispersions in ethanol. The dispersions at $c = 5 \text{ g L}^{-1}$ were remarkably stable over many months, i.e., the average size of the nanoparticles did not change, so we continued our experiments with aqueous dispersions at $c = 5 \text{ g L}^{-1}$. However, it is noteworthy that the dispersions at $c = 10 \text{ g L}^{-1}$ were also stable for a couple of days before they coagulated, allowing them to be used in processes with fast turnover times after nanoparticle synthesis.

To tackle the poor wetting of water by reducing the surface tension, we added co-solvents to the aqueous dispersions after synthesis. We had to discard the obvious choice of adding ethanol, because the faster evaporation of ethanol left us with an aqueous wet-film which again showed the common poor wetting. The azeotrope of water and ethanol would ensure the simultaneous evaporation of both agents, but it contains 96 vol% of ethanol which effectively resembles a dispersion in ethanol similar to previous studies.^[11,12]

This is why we opted for the co-solvent 2-butoxyethanol (2-BE), which is one of the state-of-the-art co-solvents in printing processes to adjust ink viscosities.^[13] The azeotrope of water and 2-BE forms at 79 vol% of water and 21 vol% of 2-BE while maintaining a convenient boiling point $T = 98.8^\circ\text{C}$, close to the boiling point of water.^[11,14] 2-BE at 21 vol% is sufficient to reduce the surface tension of the dispersion to allow coating, as evidenced by the reduction in contact angle of the dispersion on ITO/ZnO from 41° to 7° and on ITO/ZnO/P3HT:PC₇₁BM from 107° to 37° (Figure S2, Supporting Information). Not least, 2-BE has a higher viscosity (2.9 mPa s at 25°C) than water (0.89 mPa s at 25°C), which is beneficial for forming thicker wet layers during coating

and hence for reducing the number of coating steps.^[15] Importantly, the co-solvent 2-BE did not affect the stability of the nanoparticle dispersion as detailed in the Supporting Information, Table S1 and S2, Supporting Information.

2.3. Solar Cells

Finally, we fabricated P3HT:PC₇₁BM solar cells from surfactant-free nanoparticle dispersions ($c = 5 \text{ g L}^{-1}$) in a water:2-BE mixture (80:20 v/v). We varied the thickness of the light-harvesting layer between 80 and 120 nm. For this purpose, we consecutively deposited sublayers by spin coating, each with a thickness of 10 nm. In between the coating steps, we dried the layers on a hotplate (100°C , 20 s) to remove any water or 2-BE residues. After the sequential coating, the devices were annealed (150°C , 10 min) in order to connect the nanoparticles and to enhance charge carrier percolation within the layer.^[6] The light-harvesting layer was incorporated into an inverted solar cell architecture comprising ITO/ZnO/P3HT:PC₇₁BM/PEDOT:PSS/Ag on a glass substrate. All of the device fabrication and characterization were carried out inside a nitrogen glovebox. **Figure 2a** shows the current density–voltage (J – V) curves of the hero devices. All key parameters and their statistics are summarized in **Table 3**.

We found a minimum thickness of light-harvesting layers of 80 nm. Any thinner layers exhibited pinholes producing shunts. The tested devices with light-harvesting layer thicknesses between 80 and 120 nm produced power conversion efficiencies (PCEs) between 2.4 and 2.7%, which is only slightly lower than the performance of solar cells processed from ethanol-based dispersions. We speculate that the small difference in performance of solar cells fabricated from aqueous or ethanol-based dispersions stems from a somewhat different bulk-heterojunction morphology due to differences in nanoparticle packing and hence layer formation. A detailed and comprehensive study of the layer morphology after casting from water is beyond the scope of this study and will be carried out in the future.

Table 2. Average nanoparticle (NP) sizes of aqueous P3HT:PC₇₁BM (1:1 w/w) dispersions ($c = 5\text{--}10 \text{ g L}^{-1}$), measured immediately after synthesis and during storage.

Semi-conductors	Non-solvent	NP size after synthesis [nm]	NP size after 1 week [nm]	NP size after 3 weeks [nm]	NP size after 4 weeks [nm]	NP size after 6 weeks [nm]	NP size after 4 months [nm]
P3HT:PC ₇₁ BM (5 g L^{-1})	Ethanol	63 ± 1	65 ± 1	66 ± 1	65 ± 2	61 ± 2	66 ± 1
	Water	64 ± 2	64 ± 1	69 ± 1	67 ± 2	70 ± 2	70 ± 1
P3HT:PC ₇₁ BM (10 g L^{-1})	Ethanol	77 ± 1	77 ± 2	–	–	–	–
	Water	80 ± 1	120 ± 2	–	–	–	–

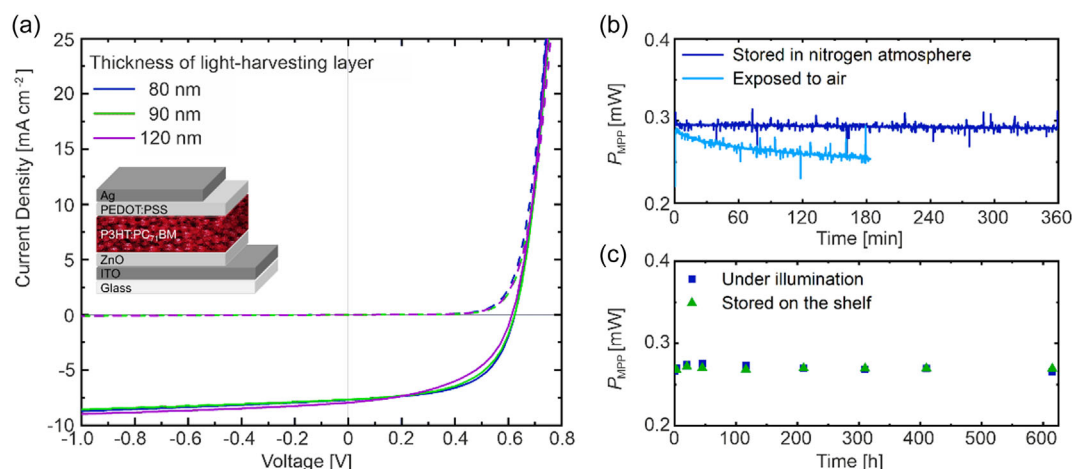


Figure 2. a) J - V curves of solar cells with P3HT:PC₇₁BM light-harvesting layers of different thicknesses (hero devices), fabricated from aqueous nanoparticle dispersions. Dashed lines represent dark curves. Inset: Device architecture. b) Power output of solar cells (thickness of the light harvesting layer: 80 nm) at the maximum power point (MPP), i.e., at a constant voltage $V_{MPP} = 470$ mV, under one-sun illumination vs. time. The solar cell that was processed, stored, and characterized in nitrogen atmosphere (dark blue line) showed almost no deterioration over 360 min. A second solar cell that was exposed to air before the measurement in nitrogen atmosphere deteriorated rather quickly. c) Power output of solar cells at MPP under illumination and stored on the shelf in the dark over 615 h, calculated from the J - V data in Figure S3, Supporting Information.

Table 3. Key parameters of solar cells with P3HT:PC₇₁BM light-harvesting layers deposited from aqueous nanoparticle dispersions.

Dispersant	Layer thickness [nm]	Deposition steps	V_{OC} [mV]	J_{SC} [mA cm ⁻²]	FF [%]	PCE [%]	Yield [no. of devices]
Water:2-BE	80	8×	622 ± 4	7.8 ± 0.1	55 ± 3	2.7 ± 0.1	15/16
	95	10×	621 ± 2	7.7 ± 0.2	55 ± 1	2.6 ± 0.1	14/16
	120	12×	612 ± 5	7.9 ± 0.1	49 ± 1	2.4 ± 0.1	14/16
Ethanol	80	6×	606 ± 2	8.0 ± 0.1	59 ± 1	2.9 ± 0.1	8/8

Whenever water is involved in organic semiconductor processes, the elephant in the room is the question of long-term stability. In Figure 2b, the power output of the solar cell with the light-harvesting layer thickness of 80 nm is depicted over time under 1-sun continuous illumination. Intriguingly, we did not observe any significant deterioration of the solar cells for the duration of 360 min as long as they were kept inside a nitrogen glovebox (dark blue line). Even illumination of the same devices over 615 h did not lead to a decrease of the solar cell performance, as shown in Figure 2c, Figure S3, S4, Table S3, S4, Supporting Information. This led us to conclude that either no water residues were left from the deposition of the light-harvesting layer or that water residues are not detrimental to the solar cell stability. Yet, we found some device deterioration, when we exposed the solar cells to ambient conditions (60 min) before the measurement in nitrogen atmosphere (Figure 2b, light blue line). In ambient conditions, we suspect oxygen to chemisorb to the ZnO transport layer, which is a well-known degradation mechanism.^[16] But overall, we conclude that the deposition of the light-harvesting layer from water does not influence the solar cells stability, rendering the processing of the light-harvesting layer from aqueous dispersions a promising concept for future solar cell production.

3. Conclusion

Organic solar cells have the potential to become all-eco-friendly and sustainable, for which the processing from nonhazardous solvents is an important cornerstone. In the past, the field progressed from chlorinated to non-chlorinated aromatic solvents and is now transforming toward processing from alcohols or water by employing nanoparticle dispersions of light-harvesting semiconductors. As of today, key to achieving high performances is the omission of surfactants. While surfactant-free dispersions in alcohols or acetonitrile have been around for two years and achieved considerable PCEs in excess of 10%, in this work, we have demonstrated that surfactant-free, aqueous dispersions can also be used for the fabrication of organic solar cells. The dispersions are stable for months, and the addition of co-solvents, such as 2-butoxyethanol, enables the wetting of surfaces even in the absence of surfactants. The PCE of 2.7% achieved in this work is higher than what has been reported in the literature so far on solar cells fabricated from surfactant-free, aqueous dispersions. Yet, it also leaves plenty of room for improvement. Better performance will only be achieved by tailoring the micro-morphology within the nanoparticles and by employing more efficient light-harvesting semiconductors. For the former, a process similar to solvent annealing (yet without employing the

common toxic chlorobenzene) will have to be developed, or a tailored functionalization of polymers must be used. For the latter, a better understanding of the stabilization mechanism of the dispersions in water in the absence of surfactants will be essential.

4. Experimental Section

All experiments were performed in a class 10 000 cleanroom.

Materials: Regioregular P3HT ("4002-EE", $M_w = 50\text{--}70\text{ kg mol}^{-1}$, regioregularity $> 90\%$) was purchased from Rieke Metals. IC₆₀BA and PC₇₁BM were purchased from Lumtec. All organic semiconductors were used without further purification. Analytical grade chloroform and analytical grade ethanol were purchased from Merck. Deionized water was further purified in an ultrapure lab-water system from Merck Millipore.

Nanoparticle Synthesis: Blends of P3HT and the fullerenes were dissolved separately in chloroform ($c = 5\text{ g L}^{-1}$) under stirring on a hotplate (47 °C) for at least half an hour. The blend solution was prepared by mixing solutions of P3HT and fullerene (1:1 w/w). Chloroform was added to the blend solution to yield the desired semiconductor concentration. For the nanoprecipitation, the P3HT:fullerene/chloroform solution (1 mL) was injected with a pipette into a beaker with the non-solvent ethanol (3 mL) under vigorous stirring. The nanoprecipitation was performed at room temperature (20 °C) and under irradiation from a chip-on-board light-emitting diode (COB-LED) with a power of 3 A (93 W).^[17] After nanoprecipitation, the beakers containing the dispersions were placed inside a water bath (47 °C) to remove the chloroform and to evaporate the excess ethanol until the initial semiconductor concentration was recovered. To remove random larger nanoparticle aggregates, which would later affect the quality of the thin film, the dispersions were centrifuged (Eppendorf, MiniSpin plus, 14 500 rpm, 1 min), and the supernatant was used for further processing. The nanoparticles were then re-dispersed in water by injecting the ethanol dispersion (1 mL) into a beaker with water (4 mL) under vigorous stirring. The re-dispersing was performed at room temperature (20 °C) under irradiation from the COB-LED. Again, the initial semiconductor concentration was recovered by evaporation of all of the ethanol and excess water inside a water bath (70 °C).

Solar Cell Fabrication: Solar cells with inverted architecture were fabricated in a glovebox under nitrogen atmosphere. For this purpose, commercially available, patterned indium tin oxide (ITO, 135 nm) coated glass substrates were wiped with glass cleaner and Q-tips. Then, they were sonicated with acetone and isopropanol (10 min each). Afterward, the substrates were exposed to oxygen plasma (120 s) to remove any organic residues from the ITO surface. An electron transport layer (10 nm) from zinc oxide nanoparticles was spin cast (2000 rpm, 40 s) onto the ITO electrode. The zinc oxide nanoparticles were synthesized following established protocols.^[18] Then the samples were dried on a hotplate (120 °C, 10 min). Light-harvesting layers were deposited by repetitive spin casting of P3HT: fullerene nanoparticle dispersions (50 μL , 60 s, and 1000 rpm) and dried on a hotplate (100 °C, 2 min) after each coating step. The complete light-harvesting layers were annealed once more on a hotplate (150 °C, 10 min). Poly(3,4-ethylenedioxythiophene):polystyrene sulfonate (PEDOT:PSS, HTL Solar, Heraeus) was spin cast (500 rpm, 3 s; 2000 rpm, 30 s; 25 nm) on top of the light-harvesting layer and annealed on a hotplate (120 °C, 10 min). Finally, a silver anode was sublimed in high vacuum (base pressure $\leq 1.10^{-6}$ mbar).

Characterization of Nanoparticle Dispersions: The intensity-based mean size distribution (hydrodynamic diameter) of the nanoparticle dispersions was determined by dynamic light scattering (DLS, Zetasizer Nano ZS, Malvern Panalytical, 20 °C) in quartz cuvettes using standard measurement protocols. The reported nanoparticle sizes and the standard deviations represent the average of 15 individual measurements of each sample. An aliquot of the dispersions in ethanol or water:2-BE was diluted in ethanol. Any solvent residues ($< 2\text{ vol}\%$) were neglected when setting up the software for these measurements. The absorbance of the dispersions was measured in two-ray transmission mode (Cary5000, Agilent Technologies) in quartz cuvettes (width 1 cm) of the same diluted

dispersions which had been used for nanoparticle size determination by DLS. All absorbance measurements were baseline corrected by simultaneous recording of the absorbance of a reference cuvette containing only the neat dispersion medium.

Characterization of Surfaces and Layers: The contact angles of the dispersions were measured using an optical contact angle goniometer (OCA25 12.40) and the drop shape analysis software (Data Physics). Glass substrates with ITO electrodes and layers of ZnO (10 nm) or layers of ZnO and nanoparticulate P3HT:PC₇₁BM were used as substrates.

All layer thicknesses were measured with a stylus profiler (Bruker, Dektak XT).

Characterization of Solar Cells: J–V curves of solar cells (photoactive area 10.5 mm²) were recorded by a source measurement unit (Keithley 2420) under irradiation from an AAA solar simulator (Xenon Sciencetech LightLine, AX-LA200, ASTM E927 AM1.5 g). For the constant illumination of the solar cells during the stability measurement over 615 h, an LED solar simulator (Oriol VeraSol-2, LSH-7320 LED, ASTM E927-05 AM1.5 g) was used. On both solar simulators, the irradiation was adjusted to a 1-sun-equivalent with a calibrated reference cell (Newport 91 150-KG5).

Supporting Information

Supporting Information is available from the Wiley Online Library or from the author.

Acknowledgements

The authors acknowledge support by the Helmholtz research program "Materials and Technologies for the Energy Transition (MTET)".

Conflict of Interest

The authors declare no conflict of interest.

Data Availability Statement

The data that support the findings of this study are available from the corresponding author upon reasonable request.

Keywords

aqueous dispersions, nanoprecipitation, organic nanoparticle dispersions, organic solar cells, surfactant-free

Received: January 12, 2025

Revised: April 8, 2025

Published online:

- [1] J. Czolk, D. Landerer, M. Koppitz, D. Nass, A. Colsmann, *Adv. Mater. Technol.* **2016**, *1*, 1600184.
- [2] K. Landfester, R. Montenegro, U. Scherf, R. Güntner, U. Asawapirom, S. Patil, D. Neher, T. Kietzke, *Adv. Mater.* **2002**, *14*, 651.
- [3] H. Laval, A. Holmes, M. A. Marcus, B. Watts, G. Bonfante, M. Schmutz, E. Deniau, R. Szymanski, C. Lartigau-Dagron, X. Xu, J. M. Cairney, K. Hirakawa, F. Awai, T. Kubo, G. Wantz, A. Bousquet, N. P. Holmes, S. Chambon, *Adv. Energy Mater.* **2023**, *13*, 2300249.
- [4] C. Xie, T. Heumüller, W. Gruber, X. Tang, A. Classen, I. Schuldes, M. Bidwell, A. Späth, R. H. Fink, T. Unruh, I. McCulloch, N. Li, C. J. Brabec, *Nat. Commun.* **2018**, *9*, 5335.
- [5] P. Marlow, F. Manger, K. Fischer, C. Sprau, A. Colsmann, *Nanoscale* **2022**, *14*, 5569.

- [6] S. Gärtner, M. Christmann, S. Sankaran, H. Röhm, E. M. Prinz, F. Penth, A. Pütz, A. E. Türel, B. Penth, B. Baumstümmler, A. Colsmann, *Adv. Mater.* **2014**, 26, 6653.
- [7] K. Fischer, P. Marlow, K. Bitsch, C. Sprau, A. Colsmann, *Sol. RRL* **2024**, 8, 2400132.
- [8] F. Manger, P. Marlow, K. Fischer, M. Nöller, C. Sprau, A. Colsmann, *Adv. Funct. Mater.* **2022**, 32, 2202566.
- [9] A. Holmes, E. Deniau, C. Lartigau-Dagron, A. Bousquet, S. Chambon, N. P. Holmes, *ACS Nano* **2021**, 15, 3927.
- [10] J. Bruder, K. Fischer, J. Armleder, E. Müller, N. Da Roit, S. Behrens, Y. Peng, W. Wenzel, H. Röhm, A. Colsmann, *Small* **2024**, 2406236.
- [11] L. H. Horsley, ed. (1 June 1973), *Azeotropic Data—III. Advances in Chemistry Series No. 166*, American Chemical Society, Washington, DC **1973**, 166.
- [12] I. S. Khattab, F. Bandarkar, M. A. A. Fakhree, A. Jouyban, *Korean J. Chem. Eng.* **2012**, 29, 812.
- [13] S. Sankaran, K. Glaser, S. Gärtner, T. Rödlmeier, K. Sudau, G. Hernandez-Sosa, A. Colsmann, *Org. Electron.* **2016**, 28, 118.
- [14] F. Quirion, L. J. Magid, M. Drifford, *Langmuir* **1990**, 6, 244.
- [15] *CRC Handbook of Chemistry and Physics*, John R. Rumble Editor-in-Chief, 104th Edition (Ed: W. M. Haynes), CRC Press/Taylor and Francis, Boca Raton, Florida **2023**, pp. 12–166.
- [16] F. Verbakel, S. C. Meskers, R. A. Janssen, *Appl. Phys. Lett.* **2006**, 89, 102103.
- [17] K. Fischer, P. Marlow, F. Manger, C. Sprau, A. Colsmann, *Adv. Mater. Technol.* **2022**, 7, 2200297.
- [18] B. Sun, H. Sirringhaus, *Nano Lett.* **2005**, 5, 2408.